EUROfusion

EUROFUSION CP(15)07/05

J. Rasmussen et al.

Investigating Fast-Ion Transport Due to Sawtooth Crashes Using Collective Thomson Scattering

14th IAEA Technical Meeting on Energetic Particles in Magnetic Confinement Systems
Vienna, Austria
(1st September 2015 – 4th September 2015)

This work has been carried out within the framework of the EUROfusion Consortium and has received funding from the Euratom research and training programme 2014-2018 under grant agreement No 633053. The views and opinions expressed herein do not necessarily reflect those of the European Commission.

Investigating fast-ion transport due to sawtooth crashes using collective Thomson scattering

J Rasmussen[1], S K Nielsen[1], M Stejner[1], B Geiger[2], A S Jacobsen[1], F Jaulmes[3], S B Korsholm[1], F Leipold[1], F Ryter[2], M Salewski[1], M Schubert[2], J Stober[2], D Wagner[2], the ASDEX Upgrade Team[2], the EUROFusion MST1 Team[4]

[1] Technical University of Denmark, Department of Physics, Fysikvej, building 309, DK-2800 Kgs. Lyngby, Denmark

[2] Max-Planck-Institut für Plasmaphysik, Boltzmannstr. 2, D-85748 Garching, Germany

[3] FOM Institute DIFFER, 3430 BE Nieuwegein, The Netherlands

[4] http://www.euro-fusionscipub.org/mst1

E-mail: `jeras@fysik.dtu.dk`

Abstract. Sawtooth instabilities can modify heating and current-drive profiles and potentially increase fast-ion losses. Understanding how sawteeth redistribute fast ions as a function of sawtooth parameters and of fast-ion energy and pitch is hence a subject of particular interest for future fusion devices. Here we present the first collective Thomson scattering (CTS) measurements of sawtooth-induced redistribution of fast ions at ASDEX Upgrade, indicating fast-ion losses in the phase-space measurement volume of about 50% across sawtooth crashes. This is in good agreement with values predicted with the Kadomtsev sawtooth model implemented in TRANSP and with the sawtooth model in the EBdyna_go code. We highlight how CTS measurements can discriminate between different sawtooth models and briefly discuss our results in light of existing measurements from other fast-ion diagnostics.

1. Introduction

Fast ions are used for heating and current drive in present-day fusion devices, and fast fusion-born α-particles will play a key role in heating the plasma in future burning-plasma machines. However, these ions can also interact strongly with a range of core-localized MHD modes, causing increased fast-ion losses and heating of the first wall [1]. Understanding the behaviour and transport of fast ions is hence important for assessing the fusion performance and stable operating regimes of future devices. One mechanism which can interact strongly with fast ions in the plasma core is the sawtooth instability [2], which redistributes heat, momentum, and particles radially outwards, including large populations of fast ions. A key challenge is to understand how this redistribution depends on fast-ion energy and pitch as well as on plasma parameters and the sawtooth crash amplitude or period.

Collective Thomson Scattering (CTS) is well suited for studies of the mechanisms underlying fast-ion redistribution by sawteeth, given its flexible measurement geometry which allows measurements in specific regions of fast-ion phase space. CTS is based on injecting an electromagnetic probe beam into the plasma and collecting part of the radiation scattered off (mainly ion-driven) fluctuations in the electron distribution. Its versatility makes CTS useful for measuring a range of parameters of both thermal and fast-ion populations [3], and a CTS system is being developed for fast α-particle measurements in ITER (e.g. [4]). In sawtooth experiments at TEXTOR, CTS was used to show that passing fast ions are more susceptible to strong sawtooth-induced redistribution than trapped fast ions [5], a result that has been subsequently confirmed using fast-ion D_α spectroscopy (FIDA) on other devices such as DIII-D [6] and ASDEX Upgrade (AUG) [7]. FIDA measurements [8, 9] have also indicated that the sawtooth redistribution of fast ions at AUG is generally well described by the widely used Kadomtsev sawtooth model [10]. Here we extend this result using CTS measurements, which are sensitive to different regions in fast-ion velocity space than FIDA.

Recently, the installation of a dedicated CTS receiver for background monitoring has helped significantly to improve the acquisition and analysis of CTS data at AUG [11]. CTS measurements of thermal and energetic ions in MHD-quiescent discharges now show good agreement with results from other diagnostics and with neo-classical theory [12]. Building on these improvements, we here present the first CTS results on fast-ion interactions with sawteeth at AUG and compare the results to predictions of the Kadomtsev model and the recently developed full-orbit code EBdyna_go [13].

2. Measurements and analysis

The results presented here are based on AUG discharge 30382, with a plasma current $I_p = 1.0$ MA, toroidal magnetic field $B_t = -2.65$ T, and a relatively low central line-integrated density $N_e \lesssim 3 \times 10^{19}$ m^{-2} (during the phase considered here). Neutral beam injection (NBI) of fast deuterium ions with the co-current on-axis NBI source Q3 (D injection energy of 60 keV) was active from $t = 2.0$–3.0 s, with no other auxiliary heating applied. As illustrated in the time traces shown in Figure 1, regular sawteeth appeared during this phase, indicated by variations in central soft X-ray data and in core ion temperature and electron density. The sawtooth crash amplitude in temperature and density is seen to remain fairly constant, whereas that of the X-ray signal rises due to an increase in the tungsten-induced radiation in the time interval considered here.

CTS data were acquired concurrently with most of the NBI phase, using the dual-receiver setup discussed in [11]. The 105 GHz probing gyrotron ($P \simeq 600$ kW, O-mode polarization) was modulated on/off in a duty cycle with 2 ms on-periods and 8 ms off-periods, to enable subtraction of the background which is dominated by electron cyclotron emission. The CTS measurement volume, defined by the overlap of the gyrotron probe beam with the receiver view, was placed slightly on the high-field side at $(R, z) = (1.62,\ 0.06)$ m. CTS measurements are sensitive to the projection of the

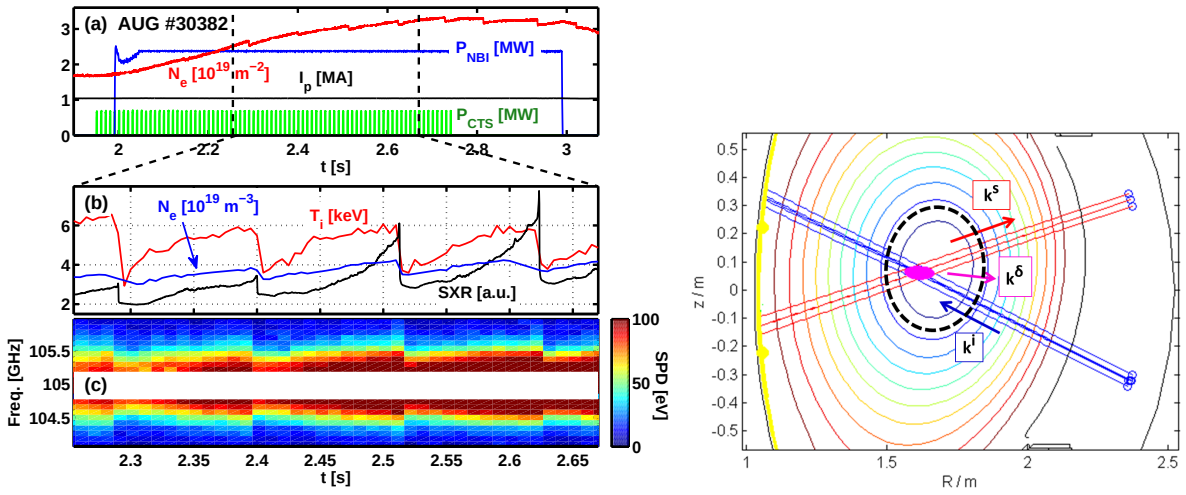

Figure 1. *Left*: Timetraces of AUG discharge 30382. (a) Central line-integrated electron density, NBI power, plasma current, and CTS probe gyrotron power. (b) Ion temperature from charge exchange recombination spectroscopy and electron density from integrated data analysis, both interpolated to the flux coordinate of the CTS volume, along with central soft X-ray signals. (c) CTS spectrogram centered on the probe gyrotron frequency, showing spectral power densities outside the stopbands of the central notch filters. *Right*: Poloidal view of the CTS scattering geometry. The incoming gyrotron probe beam (blue; wave vector $\mathbf{k}^i$) scatters off plasma fluctuations along $\mathbf{k}^\delta$ in the CTS measurement volume (magenta), to produce radiation (red; $\mathbf{k}^s = \mathbf{k}^i + \mathbf{k}^\delta$) detectable by the CTS receiver. Dashed ellipse outlines $\rho_p = 0.4$, the approximate location of the sawtooth inversion radius.

fast-ion velocity distribution function onto the plasma fluctuation vector $\mathbf{k}^\delta$, where $\mathbf{k}^\delta$ is defined by the orientation of the probe beam and receiver view (see Figure 1b). Here $\mathbf{k}^\delta$ had an angle of $\phi = \angle(\mathbf{k}^\delta, \mathbf{B}) = 101°$ relative to the local magnetic field. The measurement location corresponds to a normalized poloidal flux of $\rho_p \simeq 0.15$ and is well inside the sawtooth inversion radius at $\rho_p \approx 0.4$ as estimated from soft X-ray measurements. Indeed, the resulting background–subtracted CTS spectrogram shown in Figure 1c clearly responds to the variations in plasma properties across sawtooth crashes, with the spectra broadening during the recovery phases between crashes.

In order to interpret the observed spectral variations across sawtooth crashes, the data are analyzed using a fully electromagnetic forward model of the scattering [14]. This model employs measurements of thermal bulk plasma parameters from other diagnostics wherever available, including electron density and temperature from integrated data analysis [15] and ion temperature and toroidal rotation velocity from charge exchange recombination spectroscopy on boron, all interpolated to the flux coordinate of the measurement volume. The scattering geometry and location as estimated from raytracing are also included.

Fast ions are included in the forward model using the distribution function in the scattering volume predicted with TRANSP/NUBEAM [16], run with the Kadomtsev

model for the fast-ion redistribution at sawtooth crashes. In the TRANSP/Kadomtsev implementation, fast ions are treated in the guiding center approximation and remain bound to the evolving magnetic field lines, which undergo full reconnection during a sawtooth crash. For comparison to this, we also considered the post-crash distribution function predicted by the full-orbit EBdyna_go code [13]. In addition to assuming full Kadomtsev reconnection, this code computes the evolution of the electromagnetic fields during a sawtooth collapse based on [17] and evaluates the full particle orbits subject to these evolving fields (allowing for particle detachment from the evolving flux surfaces). To ensure a meaningful comparison with TRANSP, the EBdyna_go runs used as input the pre-crash fast-ion distribution functions predicted with TRANSP.

From fits to the measured spectra using the above scattering model, the projection of the fast-ion velocity distribution function onto $\mathbf{k}^\delta$ can also be inferred. The result is the 1D (fast) ion velocity distribution $g(u) = \int f(\mathbf{v})\delta(\mathbf{v}\cdot\mathbf{k}^\delta/k^\delta - u)\ \mathrm{d}\mathbf{v}$ in the scattering volume as a function of projected velocity u. The fitting is done within a Bayesian framework, with no functional form assumed for $g(u)$, and with uncertainties on all priors taken into account. Details on the forward modelling and the fitting procedure can be found in e.g. [12, 18].

3. Results

In Figure 2, we show measured CTS spectra before and after two sawtooth crashes at $t = 2.29$ and 2.51 s. These two crashes occur for slightly different electron densities and have different sawtooth crash durations (see Figure 1 and below). The CTS data in Figure 2 have been averaged over two gyrotron on-periods to improve the signal-to-noise ratio, giving an effective total integration time of 20 ms for CTS and background measurements. The results are compared to our forward model generated as described above, with fast ions included from TRANSP. Overall, the measurements show good agreement with the forward model. In particular, the measured spectra clearly narrow across sawtooth crashes in agreement with the model, also at frequency shifts of $\Delta f \gtrsim 0.7$ GHz from the probe gyrotron frequency, where the forward model suggests that the measurements are strongly dominated by fast ions.

At these frequency shifts, the spectral power density is seen to decrease by about 50% across the two crashes. To search for a similar effect in the fitted 1D fast-ion velocity distribution function, we compare in Figure 3 the inferred $g(u)$ to the corresponding TRANSP predictions. Following the approach in [12], TRANSP model uncertainties of 25% have also been included in the figure, based on the typical uncertainties in the kinetic profiles (N_e, T_e, T_i) inside the sawtooth inversion radius at the relevant times. Within these computational and experimental uncertainties, there is generally good agreement between TRANSP and the CTS results.

The CTS measurements clearly suggest a lower fast-ion content following the crash at $t = 2.51$ s, with indications, although less significant, of a fast-ion reduction also after the $t = 2.29$ s crash. To quantify this, we evaluate 1D partial fast-ion densities

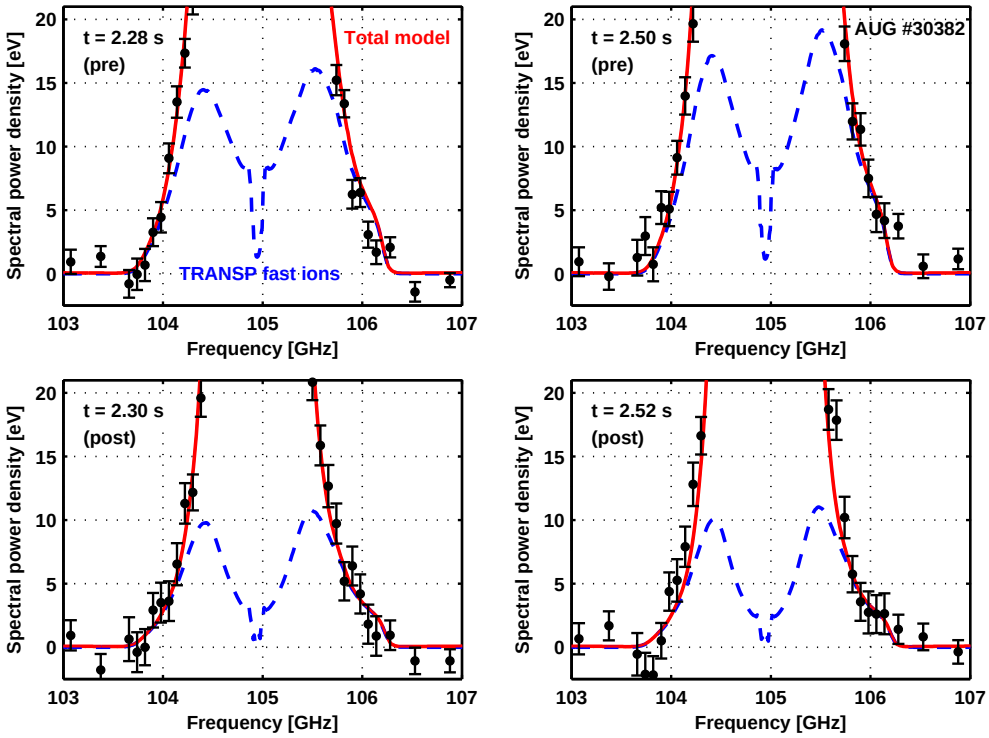

Figure 2. Pre- and post-crash CTS spectra for AUG #30382 compared to synthetic spectra from the corresponding forward model (solid red) and its fast-ion contribution from TRANSP (dashed blue) for the sawtooth crashes at (left) $t = 2.29$ s and (right) 2.51 s. Uncertainties on measured data represent the error on the mean at a given frequency within the relevant probe gyrotron pulses.

by integrating the inferred $g(u)$ across the velocity interval 1.5×10^6 m/s $< |u| < 3.5 \times 10^6$ m/s, for which both pre- and post-crash distributions are well defined by our fits. The results indicate a decrease in the fast-ion density in the observed velocity space of $40 \pm 24\%$ and $60 \pm 22\%$ at $t = 2.29$ s and 2.51 s, respectively. The quoted uncertainties here represent the propagated errors on the partial fast-ion densities, based on Monte Carlo realizations of $g(u)$ where the value of g at each velocity node u was repeatedly drawn from a Gaussian distribution with width and mean equal to the experimentally inferred value and its uncertainty, respectively. The results imply statistically significant fast-ion redistribution at levels consistent with the corresponding values of 44% and 56% predicted with TRANSP. Hence, our measurements provide the first evidence of sawtooth redistribution of fast ions measured by CTS at AUG and suggest redistribution levels which are well matched by the Kadomtsev model in TRANSP within the uncertainties.

For comparison to TRANSP, we also consider the more detailed fast-ion treatment incorporated in the EBdyna_go code, run here with sawtooth crash durations of 100 μs (at $t = 2.29$ s) and 125 μs ($t = 2.51$ s), as suggested by soft X-ray data (see [19] for details). To guide the discussion, it is instructive to first consider the simulated

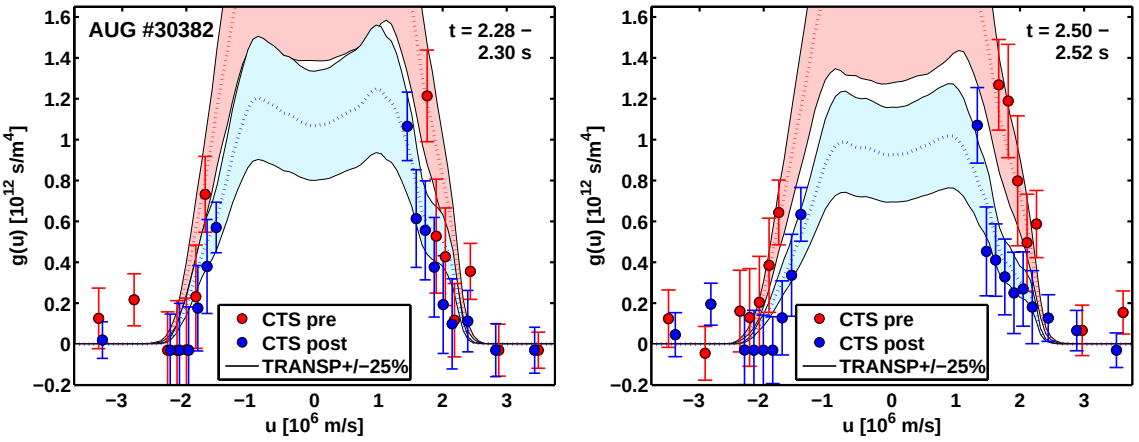

Figure 3. Fast-ion distribution functions from CTS data as a function of projected velocity before and after the sawtooth crashes at (left) $t = 2.29$ s and (right) 2.51 s. The corresponding TRANSP predictions and their uncertainties are shown as dotted lines and filled regions, respectively.

distribution function f from TRANSP and EBdyna_go around the crash times, as well as highlight some differences in the two modelling approaches. In Figure 4 we plot $f(E, p)$ in the CTS volume in energy–pitch coordinates, with pitch $p = v_\parallel/v$ (where $v_\parallel$ is the ion velocity component anti-parallel to the magnetic field, at AUG defined positive in the co-current direction). Recall that, by construction, the pre-crash distribution functions of the two codes are identical, so for EBdyna_go we only show the post-crash predictions. Also note that the EBdyna_go runs discussed here employ a coarser velocity-space grid than our TRANSP simulations, due to the computational loads associated with the full-orbit calculations. Finally, we point out that the TRANSP output has been averaged over 10 ms (to provide sufficient fast-particle statistics) and accounts for the continuous fuelling and slowing down of NBI particles during this time interval. In contrast, the EBdyna_go simulation is run at a high time resolution of a few μs, but for a shorter total duration of 0.5 ms, and includes no source or collision terms. These differences can at least partly explain the significantly higher post-crash density of ions close to the NBI injection peaks seen in the TRANSP simulation compared to EBdyna_go. While keeping this in mind, the EBdyna_go model is seen to predict a stronger overall redistribution than TRANSP at $t = 2.29$ s when integrated over fast-ion energy and pitch. However, a weaker impact on fast ions than implied by TRANSP is predicted at $t = 2.51$ s, in particular for ions with pitches close to zero (see Figure 4d).

Also shown in Figure 4 are CTS weight functions W, which illustrate the sensitivity of a CTS measurement S at a given projected velocity u and projection angle $\phi = \angle(\mathbf{k}^\delta, \mathbf{B})$ to different regions in fast-ion velocity space, such that $S = \int\int W(E,p)\, f(E,p)\, \mathrm{d}E\, \mathrm{d}p$ [4, 20]. At a projected velocity of $u = +2 \times 10^6$ m/s (but not at -2×10^6 m/s), the CTS signal is seen to contain a contribution from ions around the full-energy ($E = 60$ keV) injection peak. Even though CTS is sensitive to both

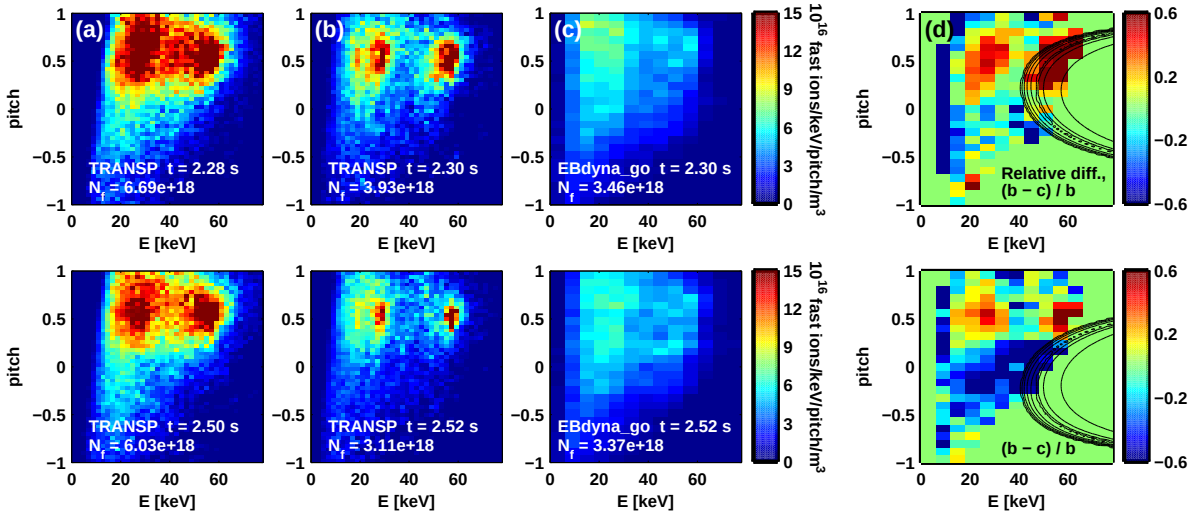

Figure 4. Fast-ion velocity distribution functions $f(E,p)$ in the CTS volume for AUG #30382, as predicted by (a) TRANSP at pre-crash, (b) TRANSP post-crash, and (c) EBdyna_go post-crash, for (top) the crash at $t = 2.29$ s and (bottom) $t = 2.51$ s. Labels give the local fast-ion density, $N_\mathrm{f} = \int\int f(E,p)\,\mathrm{d}E\,\mathrm{d}p$ [m^{-3}]. Panel (d) shows the relative post-crash difference between the models, $(f_\mathrm{TRANSP} - f_\mathrm{EBdyna\_go})/f_\mathrm{TRANSP}$, with f_TRANSP resampled to match the coarser parameter grid employed by the EBdyna_go simulation. Contours show CTS weight functions for (top) $u = +2 \times 10^6$ m/s and (bottom) $u = -2 \times 10^6$ m/s.

passing and trapped ions in the present setup ($\phi = 101°$), the central location of the CTS volume – slightly on the high-field side – implies that virtually all fast ions in the CTS volume are passing. Hence, these particular measurements cannot test the prediction of EBdyna_go that trapped and passing ions are affected differently above a certain critical energy [17] (estimated to be $E_\mathrm{crit} \approx$ 35-45 keV for the discharge and sawtooth parameters used here).

The post-crash 1D distribution functions in the CTS volume predicted by TRANSP and EBdyna_go are compared to the corresponding CTS results in Figure 5. When integrating over 1.5×10^6 m/s $< |u| < 3.5 \times 10^6$ m/s as done above, we confirm that EBdyna_go suggests a stronger fast-ion redistribution at 2.30 s than at 2.52 s (59 and 49%, respectively) in the observed velocity space, in contrast to the results from CTS and TRANSP. However, these redistribution levels remain consistent with those suggested by CTS within the uncertainties, implying that the overall redistribution inferred by CTS is in good agreement with both TRANSP and EBdyna_go.

In terms of trying to discriminate between the two codes, the situation at 2.30 s is clearly the more useful from a CTS point of view, since the stronger redistribution predicted here by EBdyna_go is reflected in a lower $g(u)$ at nearly all u. In contrast, the two model predictions at 2.52 s differ only noticeably for projected velocities corresponding to those of the thermal bulk, where $g(u)$ remains unresolved by our measurements. At 2.30 s, we note in particular the bump at $u \approx +2 \times 10^6$ m/s seen

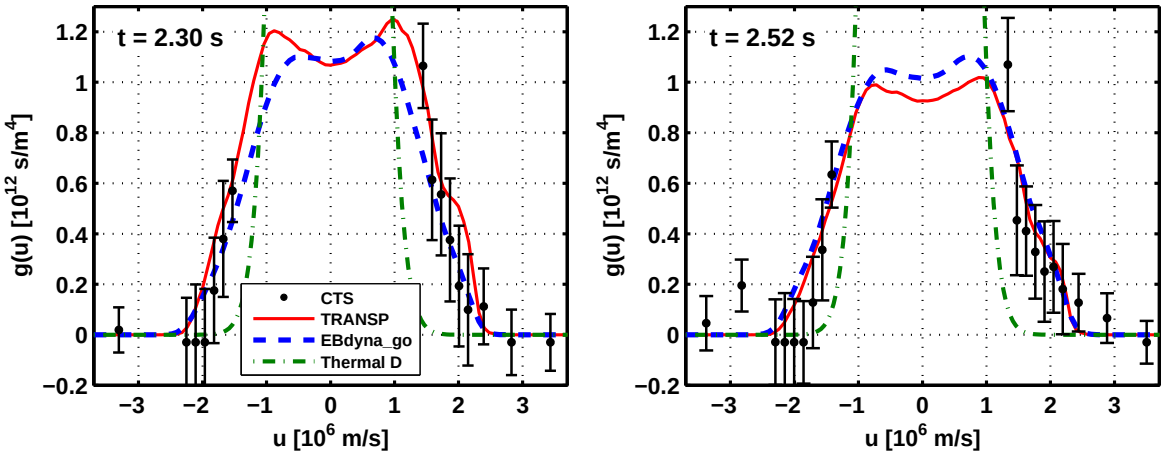

Figure 5. Comparison of the post-crash fast-ion distribution functions from CTS, TRANSP, and EBdyna_go. The thermal-ion velocity distribution function (dash-dotted) is shown for reference.

in the TRANSP model only; comparison to Figure 4d shows that this derives from the full-energy NBI peak at $E = 60$ keV, which is much more prominent in TRANSP than in EBdyna_go at post-crash. However, this difference between the two codes is mainly an artefact of the different modelling approaches as discussed above. In light of this and of the experimental uncertainties, the present data do not clearly favour one of the two sawtooth models. Future CTS data of slightly higher signal-to-noise ratio and with a scattering geometry specifically optimized for the purpose should facilitate a more robust discrimination between the different predictions.

4. Discussion and conclusions

Our CTS results across two sawtooth crashes in AUG discharge 30382 indicate a $\sim 50\%$ reduction of fast ions in the measurement volume at $\rho_p = 0.15$ in the observed velocity space, the first such CTS measurement at AUG. This finding applies to passing fast ions, which strongly dominate the measurement volume in the scattering geometry considered here. We note that no systematic variations in neutron rates are observed across the two sawtooth crashes, suggesting that most of the sawtooth-redistributed fast ions remain confined, in agreement with previous findings at AUG based on fast-ion loss detectors [7].

The observed fast-ion redistribution is found to be consistent with both the Kadomtsev model in TRANSP, thus mirroring previous results from FIDA measurements [8,9], and with the predictions of the EBdyna_go code. This represents the first demonstration of agreement between CTS sawtooth measurements and predictions of different transport codes. Further analysis and modelling of existing and forthcoming CTS sawtooth data at AUG with different scattering geometries could discriminate between the velocity-space redistribution pattern predicted by the two codes. This can test whether transport mechanisms not included in TRANSP, such as $\mathbf{E} \times \mathbf{B}$

drifts, contribute to the sawtooth–driven fast-ion redistribution in certain velocity-space regions.

In this context, we note that the CTS geometry used here is sensitive to regions in fast-ion velocity space which overlap partially with those of FIDA at AUG [12], such that signals from the two diagnostics contain a contribution from the same sub-population of fast ions. FIDA measurements in sawtooth discharges similar to AUG #30382 have recently been discussed in [8, 9]; for AUG #30815 (similar discharge parameters), these indicate a 30% fast-ion reduction on average, ranging up to 60% for strongly co-passing ions, while results for AUG #30809 (at slightly lower $B_t = -2.4$ T) suggest a central redistribution of about 50%. Our results for AUG #30382 itself are in line with these values. Work is in progress to consistently combine the FIDA and CTS fast-ion data for this discharge (Jacobsen *et al*, in prep.), in order to provide the first multi-diagnostic tomographic reconstruction [21] of the 2D velocity distribution function across a sawtooth crash. The methods and results of this work should enable a more comprehensive view of the fast-ion transport seen in these and other experiments.

Acknowledgements

This work has been carried out within the framework of the EUROfusion Consortium and has received funding from the Euratom research and training programme 2014–2018 under grant agreement No 633053. The views and opinions expressed herein do not necessarily reflect those of the European Commission.

References

[1] Gorelenkov N.N. *et al* 2014 *Nucl. Fusion* **54** 125001
[2] von Goeler S. *et al* 1974 *Phys. Rev. Lett.* **33** 1201
[3] Korsholm S.B. *et al* 2010 *Nucl. Instrum. Methods Phys. Res. A* **623** 677
[4] Salewski M. *et al* 2011 *Nucl. Fusion* **51** 083014
[5] Nielsen S.K. *et al* 2011 *Nucl. Fusion* **51** 063014
[6] Muscatello C.M. *et al* 2012 *Plasma Phys. Control. Fusion* **54** 025006
[7] Geiger B. *et al* 2014 *Nucl. Fusion* **54** 022005
[8] Geiger B. *et al* 2015 *Nucl. Fusion* **55** 083001
[9] Geiger B. *et al* 2015 *Plasma Phys. Control. Fusion* **57** 014018
[10] Porcelli F. *et al* 1996 *Plasma Phys. Control. Fusion* **38** 2163
[11] Nielsen S.K. *et al* 2015 *Plasma Phys. Control. Fusion* **57** 035009
[12] Rasmussen J. *et al* 2015 *Plasma Phys. Control. Fusion* **57** 075014
[13] Jaulmes F. *et al* 2014 *Nucl. Fusion* **54** 104013
[14] Bindslev H. 1996 *J. Atmos. Terr. Phys.* **58** 983–9
[15] Fischer R. *et al* 2010 *Fusion Sci. Technol.* **58** 675-84
[16] Pankin A. *et al* 2004 *Comp. Phys. Comm.* **159** 157–84
[17] Kolesnichenko Ya.I. and Yakovenko Yu.V. 1996 *Nucl. Fusion* **36** 159
[18] Salewski M. *et al* 2010 *Nucl. Fusion* **50** 035012
[19] Jaulmes F. *et al* 2015 *These proceedings*
[20] Heidbrink W.W. *et al* 2007 *Plasma Phys. Control. Fusion* **49** 1457-1475
[21] Salewski M. *et al* 2013 *Nucl. Fusion* **53** 063019